Sains Malaysiana 51(7)(2022): 2097-2118
http://doi.org/10.17576/jsm-2022-5107-13

DFT and CBS Study of Ethyl Acetate Conformers in the Neutral Hydrolysis

(Kajian DFT dan CBS terhadap Konformer Etil Asetat dalam Hidrolisis Neutral)

VERA KHOIRUNISA[1,2], FEBDIAN RUSYDI[3,4,*], ROICHATUL MADINAH[4,5], HERMAWAN KRESNO DIPOJONO[1], FAOZAN AHMAD[6], MUDASIR[7], IRA PUSPITASARI[4,8] & AZIZAN AHMAD[5]

[1]*Department of Engineering Physics, Faculty of Industrial Technology, Institut Teknologi Bandung, Jl. Ganesha no. 10, Bandung 40132, Indonesia*
[2]*Engineering Physics Study Program Institut Teknologi Sumatera, Jl. Terusan Ryacudu Lampung Selatan 35365, Indonesia*
[3]*Department of Physics, Faculty of Science and Technology, Universitas Airlangga, Jl. Mulyorejo, Surabaya 60115, Indonesia*
[4]*Research Center for Quantum Engineering Design, Faculty of Science and Technology Universitas Airlangga, Jl. Mulyorejo, Surabaya 60115, Indonesia*
[5]*Department of Chemical Sciences, Faculty of Science and Technology, Universiti Kebangsaan Malaysia, 43600 UKM Bangi, Selangor Darul Ehsan, Malaysia*
[6]*Department of Physics, Faculty of Mathematics and Science, Institut Pertanian Bogor, Bogor 16680, Indonesia*
[7]*Department of Chemistry, Faculty of Mathematics and Science, Universitas Gadjah Mada, Yogyakarta 55281, Indonesia*
[8]*Information System Study Program, Faculty of Science and Technology, Universitas Airlangga, Jl. Mulyorejo, Surabaya 60115, Indonesia*

Received: 28 August 2021/ Accepted: 12 January 2022

ABSTRACT

First-principles calculations are commonly used to search for possible transition states in reaction kinetics studies, which are such a challenge to observe experimentally. However, computationally studying the reaction is also challenging because of, inter alia, the Basis Set Incompleteness Error (BSIE). Accordingly, we utilized density functional theory-based calculations and the complete basis set method, to confirm the conformational effect in the neutral hydrolysis of three ethyl acetate analogs: ethyl formate, ethyl acetate, and ethyl fluoroacetate. The results showed that both methods yielded activation energy span, which implies that the conformational effect in the ethyl acetate neutral hydrolysis is not due to the BSIE. The results also demonstrated the importance of polarization and diffuse function in a basis set. The former was to improve the ground state geometry, and the latter was to increase the activation energy.

Keywords: Complete basis set; conformational effect; density functional theory; energy; neutral hydrolysis

ABSTRAK

Pengiraan prinsip pertama biasanya digunakan untuk mencari kemungkinan keadaan peralihan dalam kajian kinetik tindak balas, yang merupakan satu cabaran untuk diperhatikan secara uji kaji. Walau bagaimanapun, mengkaji reaksi secara komputasi juga mencabar kerana antara lain Set Asas Ketaklengkapan Ralat (BSIE). Oleh kerana itu, kami melakukan pengiraan berdasarkan teori fungsi ketumpatan dan set asas lengkap, untuk mengesahkan kesan konformasi pada hidrolisis netral tiga analog etil asetat: etil format, etil asetat dan etil fluoroasetat. Hasil kajian menunjukkan bahawa kedua-dua kaedah menghasilkan rentang tenaga pengaktifan, yang menunjukkan bahawa kesan konformasi dalam hidrolisis netral etil asetat bukan disebabkan oleh BSIE. Hasilnya juga menunjukkan pentingnya fungsi polarisasi dan difusi dalam set asas dengan teori fungsi ketumpatan untuk mendapatkan geometri keadaan asas yang lebih tepat dan set asas lengkap untuk meningkatkan tenaga pengaktifan.

Kata kunci: Hidrolisis neutral; kesan konformasi; set asas lengkap; tenaga; teori fungsi ketumpatan

INTRODUCTION

First-principles calculations have been common methods to study the reactivity of a molecule (Cameron & Amir 2019; Febdian et al. 2019; Fei et al. 2015; Hossein et al. 2019; Hui et al. 2019; Nina et al. 2015). Coupled with vibrational mode calculations, the method allows us to determine activation energy at a certain temperature, which is the most significant quantity in a reactivity study. Activation energy calculations require transition state information, which is a challenge to acquire experimentally.

A first-principles study on reactivity is not an easy task despite the rapid development of quantum chemistry software. The calculations may cause false alarms due to its intrinsic errors from the mathematical approximations, such as the Basis Set Incompleteness Error (BSIE) arising from basis set truncation. The BSIE triggers another intrinsic error: Basis Set Superposition Error (BSSE) (Roman 2010). The BSIE affects significantly when two molecules are held together by a non-covalent interaction (Angel et al. 2019; Yuan et al. 2013). The non-covalent interaction often exists in an activated complex, in a transition state. Moreover, the basis set may affect the geometrical structure and vibrational modes, which consequently affects the activation energy calculations (Jae & Young 2014; Johannes et al. 2016; Venkatesan et al. 2012).

Conformation, like other stereochemistry features of molecules, influences the molecule's reactivity (Francis & Richard 2007; Hussein et al. 2020; Nadezhda et al. 2016). Early application of conformational analysis on reactivity problems dates back about seventy years ago to understand the esterification of four menthol isomers (Ernest 1953) built upon experimental results from nearly ninety years ago (John & William 1934). Aside from menthol isomers, the same effect appears in ester hydrolysis (Johannes et al. 1997; Pierre 1975; Radhakrishnamurti & Prakash 1970). Even though the conformational analysis has been used for a long time, it still attracts considerable interest to date (Simone et al. 2019; Toby et al. 2017; Vladimir & Nediljko 2018; Weck et al. 2019). Our previous study (Febdian et al. 2019) on ethyl acetate neutral hydrolysis resulted in the span of activation energy due to the effect of conformers that is about 3.5 kcal/mol by using Density Functional Theory (DFT) (Pierre & Walter 1964; Walter & Lu 1965). The energy value is the typical value of BSSE (Rincón et al. 2016; Santanu et al. 2018), which is triggered by BSIE. In our other study on acetylcholine, an ester family but in a more complex structure than ethyl acetate, the activation energy of its hydrolysis was even higher, 8.1 kcal/mol (Rizka et al. 2020). Considering these findings, confirming the conformational effect in ethyl acetate neutral hydrolysis is necessary.

This work is the first attempt to confirm the conformational effect in ethyl acetate neutral hydrolysis. We employed DFT and Complete Basis Set (CBS) (Petersson et al. 1988) methods to estimate the BSIE through their results' comparison. While it was expected that this approach would be able to estimate the BSIE, to the best of our knowledge, there was no study that uses the CBS method for the case of ethyl acetate neutral hydrolysis. The cases selected in this work were the neutral hydrolysis of three ethyl acetate analogs, which are ethyl formate, ethyl acetate, and ethyl fluoroacetate. We also varied the basis sets in the DFT method to verify the effect of polarization and diffuse function being sought in this study. The former method is to verify the effect of polarization and diffuse function, while the latter is for the effect of long-range and dispersion interaction being sought in this study. Overall, this study would answer the following questions: (a) how BSIE affects the conformational effect in ethyl acetate neutral hydrolysis? and (b) how polarization and diffuse function contributes to the calculation results?.

MATERIALS AND METHODS

We adopted the exact reaction model (Scheme 1), the nomenclature system (Table 1 & Figure 1), as well as the thermochemistry calculation method from our previous study (Febdian et al. 2019). The molecules of interest are three ethyl acetate analogs (Et analog), which are (i) ethyl formate (R is H), (ii) ethyl acetate (R is CH3), and (iii) ethyl fluoroacetate (R is CH2F). In the transition state, the ester and water form an [Et analog–water] activated complex. We focused on two conformers of each molecule, the ones with the highest and the lowest rate constant as calculated in our previous study (Febdian et al. 2019).

TABLE 1. The nomenclature system used throughout the manuscript

Molecule	Label	(numbering)	Conformation
Ethyl formate	Et1	(1)	trans
		(2)	gauche
Ethyl acetate	Et2	(1-a)	trans R′ with eclipsed R
		(2-d)	gauche R′ with staggered R
Ethyl fluoroacetate	Et3	(1-d)	trans R′ with staggered R, where F atom is at "d"
		(2-e)	gauche R′ with staggered R, where F atom is at "e"

Note: The nomenclature system is adopted from our previous study

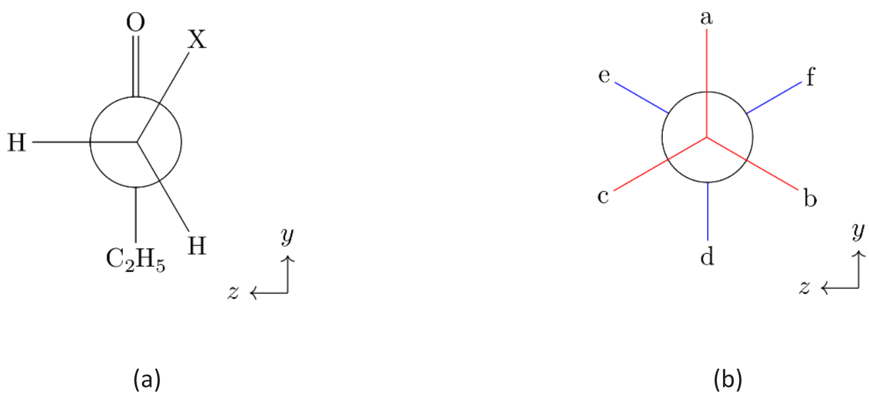

FIGURE 1. (a) The general Newman projection along C1-C4 bond for ethyl acetate derivatives in this study, (b) The position "X" defines the eclipse (a, b, and c) and the staggered (d, e, and f) conformations. The "X" is H in Et2 and is F in Et3

RCO-OR'	+	H_2O	→	[ester-water]	→	RCO-OH	+	H-OR'
Et analog		water		transition state		carboxylic acid		alcohol

SCHEME 1

We employed two different calculation methods for the ground, and the transition states optimization in Scheme 1. The first method was DFT with B3LYP, CAM-B3LYP (Takeshi et al. 2004), and M06-2X (Yan & Donald 2008) functional. We used B3LYP with six different basis sets (M1–M6); while CAM-B3LYP (M8) and M06-2X (M9) were with the 6-311++G(d,p), which was the basis set in our previous study (Febdian et al. 2019) (Table 2). The second method was CBS-APNO (M7), with its basis set component being 6-311G(d,p) (Joseph et al. 1996). We defined M1-M7, which differed in basis set, as cluster A and M6-M9, which differed in exchange-correlation functional, as cluster B. Since the CBS method significantly reduces the BSIE (Juan & Annia 2010), comparing results from these two computational methods will illustrate the BSIE's significance in the energy barrier calculations.

TABLE 2. The calculation methods used in this study

Method	Label	Description
B3LYP/STO-3G	M1	Pople basis set: Slater-type orbital consisting of three Gaussian-type orbitals
B3LYP/6-31G	M2	Pople basis set: Gausian-type orbital, split valence double zeta basis set
B3LYP/6-31G(d,p)	M3	Pople basis set: M2 with the addition of polarization functions
B3LYP/6-31++G(d,p)	M4	Pople basis set: M3 with the addition of diffuse functions
B3LYP/aug-cc-PVDZ	M5	Dunning's basis set which has the same amount of basis functions with M4
B3LYP/6-311++G(d,p)	M6*	Pople basis set: M4, split valence triple zet basis set
CBS-APNO	M7	Compound method with geometry optimization based on QCISD/6-311G(d,p), and energy extrapolation using QCIST(T), HF, and MP2.
CAM-B3LYP/6-311++G(d,p)	M8*	Exchange-correlation functional with long-range corrections
M06-2X/6-311++G(d,p)	M9	Exchange-correlation functional with corrections for non-covalent interactions

Note: *The method used in our previous study (Febdian et al. 2019)

We also used the optimized structures from the previous study as the initial guess, as shown in Figure 2 (for the ground state) and Figure 3 (for the transition state), and applied the same calculation routines (Febdian et al. 2021, 2019) using Gaussian 16 software (Frisch et al. 2016).

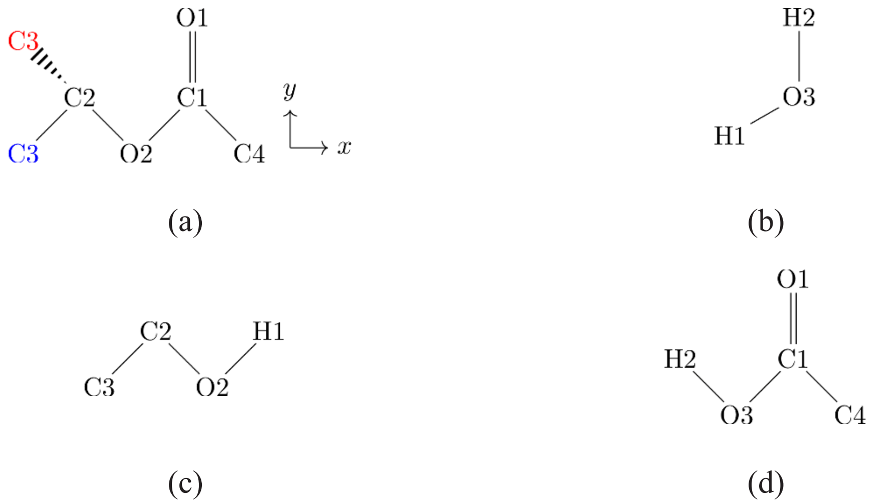

FIGURE 2. The molecular model (a) Et2, (b) water, (c) ethanol, and (d) acetic acid. The position of C3 of Et2 determines the conformation: gauche (red) or trans (blue)

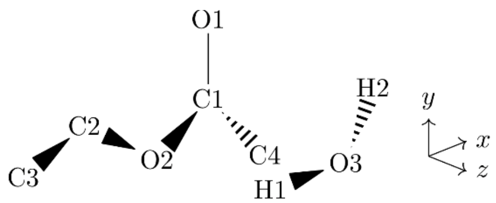

FIGURE 3. The molecular model of transition state structure, which is an activated complex of [ethyl acetate – water]. C1-O3 is in z-axis

Results and Discussion

TRANS–ETHYL ACETATE IN THE GROUND STATE

We used trans–ethyl acetate [Et2(1–a)] for assessing the ground spin state in all methods. All methods agreed that the ground spin state is singlet as shown in Table 1. It was noteworthy that the energy difference between triplet and singlet spin states, ΔE_{13}, can be classified into two groups: lower than +4.08 eV (M1 and M2) and higher than +4.08 eV (M3 to M9). If we eliminate the first group, the average of ΔE_{13} changed from +4.08 eV to +4.25 eV, and the span decreased from +1.36 eV to +0.26 eV. The decreasing span indicates that the accuracy level of M1 and M2 is significantly different from other methods.

At the ground spin state, not all methods yielded good accuracy with respect to the experimental data. The justification of the accuracy is based on Young (2001). Table 3 shows the geometrical parameters of the ester's core. The Cartesian coordinates of the optimized geometries are given in the electronic supplementary materials (Table S1-S12). The accuracy level of M1 and M2 was significantly different from experimental data (Kozo et al. 1998; William 2015), as it was in the case of ΔE_{13}. Even for the water molecule, M1 and M2 results were significantly off. Therefore, M1 and M2 are not suitable to use in this study.

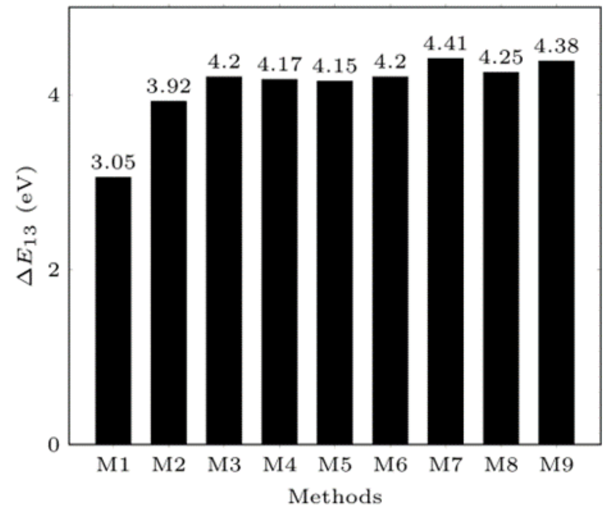

FIGURE 4. The energy difference (ΔE_{13}) between singlet and triplet spin state of trans ethyl acetate. (ΔE_{13}) is the values of $E_{triplet}$ - $E_{singlet}$. The positive value shows that $E_{triplet}$ is higher than $E_{singlet}$

TABLE 3. The geometrical parameters of ethyl acetate's core (O2−C1=O1) and water (H1−O3−H2) in the ground state. Parameter R(X,Y) is the bond distance of X−Y (Å), A(X, Y, Z) is the bond angle of X−Y−Z (deg.), and Δ is the absolute value of Expr. − Calc. difference

	Parameter	Expr.	M1		M2		M3		M4		M5		M6		M7		M8		M9	
			Calc.	Δ	Calc.	Calc.	Δ	Calc.	Δ	Calc.	Δ	Calc.	Δ	Calc.	Δ	Calc.	Δ	Δ	Calc.	Δ
(a)	Ethyl acetate																			
	R(C1,O1)	1.203	1.250	0.047	1.236	1.215	0.012	1.213	0.01	1.203	0.000	1.201	0.002	1.207	0.004	1.205	0.002	0.033	1.212	0.009
	R(C1,O2)	1.345	1.431	0.086	1.377	1.353	0.008	1.354	0.009	1.343	0.002	1.343	0.002	1.351	0.006	1.351	0.006	0.032	1.353	0.008
	A(C4,C1,O2)	110.8	108.6	2.2	111.2	111.2	0.4	111.2	0.4	111.3	-0.5	111.2	-0.4	111	0.2	110.6	0.2	0.4	110.8	0.0
	A(C1,O2,C2)	117.3	110.1	7.2	117.2	116.5	0.8	116.2	1.1	116.5	0.8	115.9	1.4	116.6	0.7	114.9	2.4	0.1	115.8	1.5
(b)	Water																			
	R(O3,H1)	0.958	1.027	0.069	0.976	0.965	0.007	0.965	0.007	0.960	-0.002	0.959	-0.001	0.962	0.004	0.957	0.001	0.018	0.965	0.007
	A(H1,O3,H2)	104.5	97.2	7.3	108.3	105.7	1.2	104.7	0.2	105.5	-1.0	105.1	-0.6	105	0.5	102.7	1.8	3.8	103.7	0.8

Among the results of all methods that yield good accuracy, the one of M7 differed. The discrepancy of M7's prediction on A(C1,O2,C2) with respect to the experiment was more than 2Å, while the rest was below that. The same pattern occurred on the prediction of ethyl acetate's bond angle A(H1,O3,H2). It is due to the geometrical optimization of M7 which was performed using QCISD/6-311G(d,p), which does not have a diffuse function in the basis set. Compared to M3 [B3LYP/6-31G(d,p)] which also does not have a diffuse function, the error predicted by M7 is still larger. It is due to the nature of QCISD which works based on wave function, while DFT works based on density. Therefore, the sensitivity of QCISD on the choice of basis set is higher than DFT. The geometrical accuracy of the ester's core showed the importance of polarized basis set function. It was the property that was shared by all suitable calculation methods, from M3 to M9. The change in exchange-correlation functional from B3LYP (M3–M5) to CAM-B3LYP (M8) and to M06-2X (M9) did not give significant effect. It was in line with NBO calculation results which show the presence of lone pairs in O_1 and O_2 of ester's core. It has been known that the lone pair requires the polarization function in the basis set.

In detail, the results of cluster A (M1-M7) showed that the overall accuracy of M5 fell between M4 and M6. It indicated that the correlation-consistent factor in Dunning's basis set could overcome the number of zeta functions in the Pople basis set. Meanwhile, the result of cluster B (M6-M9) showed that the four methods were comparable. The corrections provided by M7-M9 did not significantly affect ethyl acetate analogs' ground state structure. It indicated the dominance of covalent interactions that dwarfed the non-covalent ones.

Table 4 shows the charge population from the suitable calculation methods. All suitable methods agreed that the electrophilic site was at C1. The result agreed with the established knowledge of ester that the electrophilic site is indeed at C1.

The charge population yielded by M7 showed a distinct result compared to M3-M6 and M8-M9. M7 predicted a more negative charge population of Oxygen but a more positive one of Carbon atoms compared to another method. In case of C1, the electrophilic site, M7 predicted the charge population being 0.945, while the rest was around 0.825 (in average). It may cause M7 to predict the distance of C1 and O3 of water in the transition state being shorter compared to the other methods.

TABLE 4. The charge population (in unit e) of ethyl acetate in the ground state

Atom	M3	M4	M5	M6	M7	M8	M9
O1	-0.599	-0.611	-0.629	-0.6	-0.684	-0.609	-0.607
O2	-0.566	-0.573	-0.593	-0.575	-0.622	-0.580	-0.591
C1	0.828	0.815	0.847	0.809	0.945	0.822	0.831
C2	-0.122	-0.113	-0.087	-0.034	0.008	-0.039	-0.036
C3	-0.711	-0.681	-0.659	-0.59	-0.546	-0.598	-0.599
C4	-0.786	-0.75	-0.725	-0.668	-0.642	-0.677	-0.678

STRUCTURES IN THE TRANSITION STATE

All suitable calculation methods agreed that the structures in the transition state were generally alike. They shared the same property: The elongation of R(C1,O2) and R(O3,H1) as shown in Table 5. The Cartesian coordinates of the optimized transition state structures are given in the electronic supplementary materials (Table S13-S24). A correct transition state requires these elongations so that the breaking of C1−O2 and O3−H1 can begin to form the product. It implies that M3 to M9 can predict the correct transition state.

Even though the transition state structures were generally alike, the detailed geometrical parameters calculated by M7 were significantly different among the methods in cluster A. First, the elongation of C1−O2 by M7 was the shortest. For example, in the [Et2-water] case, while M3 to M6 predicted that the elongation was longer than 0.41 Å, the CBS method (M7) predicted it at only 0.37 Å. Second, the distance of C1−O3 by M7 (Table 5) was also the shortest. It aligns with the aforementioned discussion on the atomic charge population.

The significant difference in the detailed geometrical parameters also appeared in cluster B. The comparison of M6–M9 showed the significance of non-orbital interactions in the transition state in which the four methods (B3LYP, CAMB3LYP, M06-2X, and CBS) treated it differently. To be specific, comparing M6, M8, M9 (DFT) with M7 (CBS) suggests that BSIE plays a role in the transition state optimization.

THE ACTIVATION ENERGY

Table 6 shows the standard Gibbs energy of activation ($\Delta^{\ddagger}G°$) from all hydrolysis cases as determined by all suitable calculation methods. All methods with diffused basis sets calculated $\Delta^{\ddagger}G°$ to be higher than 51.0 kcal/mol, while M3 predicted it at about 46 kcal/mol. It indicates the significant effect of diffuse function in the basis set is suitable for this research paradigm.

TABLE 5. The selected parameter in the ([Et*n*-water]) complex with 'elng'. Refers to the difference between in the transition and in the ground state (Table 3)

Conformer	M3	elng.	M4	elng.	M5	elng.	M6	elng.	M7	elng.	M8	elng.	M9	elng.
[Et1-water]														
C1-O2														
(1)	1.716	0.375	1.697	0.356	1.713	0.371	1.715	0.376	1.670	0.333	1.663	0.332	1.649	0.317
(2)	1.713	0.371	1.699	0.357	1.713	0.370	1.720	0.380	1.674	0.332	1.668	0.336	1.651	0.318
O3-H1														
(1)	1.208	0.243	1.231	0.266	1.231	0.266	1.236	0.274	1.210	0.253	1.232	0.271	1.224	0.265
(2)	1.210	0.245	1.224	0.259	1.228	0.263	1.227	0.265	1.204	0.247	1.221	0.261	1.217	0.258
C1-O3														
(1)	1.730		1.754		1.770		1.780		1.713		1.731		1.707	
(2)	1.731		1.750		1.769		1.773		1.706		1.724		1.701	
[Et2-water]														
C1-O2														
(1-a)	1.777	0.424	1.765	0.412	1.780	0.426	1.791	0.440	1.722	0.371	1.727	0.384	1.701	0.358
(2-d)	1.774	0.420	1.765	0.411	1.780	0.425	1.793	0.441	1.721	0.369	1.726	0.382	1.701	0.357
O3-H1														
(1-a)	1.202	0.237	1.225	0.260	1.227	0.262	1.228	0.266	1.210	0.253	1.224	0.264	1.225	0.266
(2-d)	1.205	0.240	1.223	0.258	1.226	0.261	1.225	0.263	1.204	0.247	1.223	0.263	1.217	0.258
C1-O3														
(1-a)	1.780		1.810		1.829		1.841		1.755		1.780		1.756	
(2-d)	1.781		1.810		1.828		1.838		1.748		1.780		1.747	
[Et3-water]														
C1-O2	1.713	0.377	1.680	0.347	1.697	0.362	1.695	0.364	1.653	1.636	0.297	1.628	0.304	1.636
(1-d)	1.708	0.370	1.694	0.360	1.709	0.374	1.713	0.382	1.655	1.704	0.365	1.675	0.337	1.704
(2-e)														
O3-H1	1.209	0.244	1.224	0.259	1.227	0.262	1.234	0.272	1.211	1.223	0.263	1.223	0.264	1.223
(1-d)	1.225	0.26	1.252	0.287	1.252	0.287	1.256	0.294	1.226	1.201	0.241	1.204	0.245	1.201
(2-e)														
C1-O3	1.729		1.733		1.753		1.760		1.696	1.695		1.688		1.695
(1-d)	1.757		1.797		1.815		1.824		1.729	1.718		1.690		1.718
(2-e)	1.713	0.377	1.680	0.347	1.697	0.362	1.695	0.364	1.653	1.636	0.297	1.628	0.304	1.636

TABLE 6. The standard Gibbs energy of activation (kcal/mol) from all conformers

Conformer	M3	M4	M5	M6	M7	M8	M9
[Et1-water]							
$\Delta^{\ddagger}G°$							
(1)	47.62	51.65	52.22	52.93	54.18	53.29	52.98
(2)	46.31	51.28	51.6	52.21	53.71	52.44	51.51
Span	1.31	0.37	0.62	0.72	0.47	0.85	1.48
[Et2-water]							
$\Delta^{\ddagger}G°$							
(1-a)	47.52	52.88	52.85	53.52	53.68	54.01	52.92
(2-d)	46.64	51.90	52.07	52.45	53.01	53.05	52.69
Span	0.88	0.98	0.78	1.07	0.67	0.97	0.23
[Et3-water]							
$\Delta^{\ddagger}G°$							
(1-d)	47.35	53.60	54.01	54.86	54.00	54.97	52.78
(2-e)	46.32	51.42	51.88	52.22	52.76	52.57	51.73
Span	1.03	2.18	2.13	2.64	1.24	2.40	1.05

The trend in the ground and the transition state geometries (Tables 3 & 5, respectively) also appeared in the $\Delta^{\ddagger}G°$. First, M5's results fell between M4's and M6's results. It shows the robustness of the DFT method for the ground and the transition state optimization. Second, M7's results were overall the highest. It implies that the BSIE lowers the $\Delta^{\ddagger}G°$ in the DFT calculations.

Another remarkable trend was related to the halogenation effect. Our previous study (Febdian et al. 2019) found that halogenation decreases the $\Delta^{\ddagger}G°$, except for the halogenation at the staggered 1-d conformation (Figure 1). The pattern remained: halogenation decreased the $\Delta^{\ddagger}G°$, except for the 1-d conformation, despite the changes in the basis set (M3 to M6), the use of CBS method (M7), the changes in exchange-correlation functional (M8 and M9). Since the rate constant was exponentially proportional to the negative $\Delta^{\ddagger}G°$, we find consistency in the suitable calculation methods regarding halogenation effect: it will increase the value of rate constant, which agreed with the experimental observations (Arlo & Herschel 1959; Erkki & Nils 1963; Venkatasubban et al. 1978).

Table 6 also shows the sensitivity of the method towards the size of the molecules. M4-M6 and M8 were more sensitive than M7 and M9. The difference on the value of $\Delta^{\ddagger}G°$ among the three systems predicted by M7 and M9 was less than 1 kcal/mol, which is below the chemical accuracy. Along with the fact that (i) M7 and M9 deal with errors due to the BSIE and dispersion effect and (ii) the three systems which do not significantly differ, the results show the significance of BSIE and dispersion correction in B3LYP exchange-correlation's prediction. Overall, the value of $\Delta^{\ddagger}G°$ predicted by M6-M9 was comparable. The difference was around 1 kcal/mol for each system. It indicates that both DFT and CBS were suitable for this study. The span of $\Delta^{\ddagger}G°$ resulted by both methods confirms the conformational effect in the transition state, as reported in our previous study (Febdian et al. 2019).

Conclusion

We have confirmed the conformational effect in the neutral hydrolysis of ethyl acetate analogs, which were ethyl formate, ethyl acetate, and ethyl fluoroacetate. The strategy was to capture the effect as an activation energy span, which is the discrepancy between the maximum and the minimum value, using DFT and CBS. Both methods yielded comparable results, which were around two and one kcal/mol for DFT and CBS, respectively. The span comparison suggests a larger BSIE in DFT-based calculation than in CBS; but both methods confirm the existence of conformational effect in the neutral hydrolysis.

In addition, we demonstrated the importance of polarization and diffuse function in the basis set for this study. The former improved the ground state geometry accuracy, and the latter altered the activation energy calculation significantly. Without the polarization function in the basis set, the DFT method's error on the ground state geometry could be up to 0.08 Å with respect to the experimental data. The diffuse function in the basis set increased the activation energy by around 3 kcal/mol. It is important to note that, while the CBS method calculated the activation energy differently from the DFT method, their estimations on geometries at the ground and the transition state were comparable.

ACKNOWLEDGEMENTS

The authors wish to thank Prof. Ryo Maezono and Prof. Kenta Hongo (Japan Advanced Institute of Science and Technology, Japan), Prof. Heni Rachmawati (Institut Teknologi Bandung, Indonesia), Rizka N. Fadilla (Osaka University, Japan), Nufida D. Aisyah, Lusia S. P. Boli, and Dr. Adhitya G. Saputro (Institut Teknologi Bandung, Indonesia) for the valuable discussion. All calculations using Gaussian 16 software were performed in Riven, the computer facility at Research Center for Quantum Engineering Design, Universitas Airlangga, Indonesia. This work was supported by Direktorat Riset dan Pengabdian Masyarakat, Deputi Bidang Penguatan Riset dan Pengembangan Kementerian Riset dan Teknologi/Badan Riset dan Inovasi Nasional, Republik Indonesia under grant scheme Penelitian Dasar Unggulan Perguruan Tinggi (PDUPT) 2021 No. 451/UN3.15/PT/2021. Supplementary information for this paper is provided and available online. The authors contributions is as follows: Conceptualization, methods: Febdian Rusydi; formal analysis: Vera Khoirunisa, Faozan Ahmad, Mudasir, Ira Puspitasari; investigation: Vera Khoirunisa, Roichatul Madinah; writing–original draft preparation: Vera Khoirunisa, Roichatul Madinah; and writing–review and editing: Febdian Rusydi, Hermawan K. Dipojono, and Azizan Ahmad. All authors have read and agreed to the published version of the manuscript.

REFERENCES

Angel, V., Luis, C.V.P., Olalla, N.F. & Carlos, S.L. 2019. On the use of popular basis sets: Impact of the intramolecular basis set superposition error. *Molecules* 24: 3810.

Arlo, M. & Herschel, H. 1959. Solvent and chain length effects in the non-catalyzed hydrolysis of some alkyl and aryl trifluoroacetates. *Journal of the American Chemical Society* 81: 2082-2086.

Cameron, D.S. & Amir, K. 2019. Kinetics and thermodynamics of reactions involving criegee intermediates: An assessment of density functional theory and *ab initio* methods through comparison with CCSDT(Q)/CBS data. *Journal of Computational Chemistry* 41: 328-339.

Erkki, K.E. & Nils, J.C. 1963. Kinetics of the neutral hydrolysis of chloromethyl chloroacetate. *Acta Chemica Scandinavica* 17: 1584-1594.

Ernest, L.E. 1953. The origin of steric hindrance in cyclohexane derivatives. *Experientia* 9: 91-93.

Febdian, R., Roichatul, M., Ira, P., Wun, F.M., Azizan, A. & Andrivo, R. 2021. Teaching reaction kinetics through isomerization cases with the basis of density-functional calculation. *Biochemistry and Molecular Biology Education* 49: 216-227.

Febdian, R., Nufida, D.A., Rizka, N.F., Hermawan, K.D., Faozan, A., Mudasir, Ira, P. & Andrivo, R. 2019. The transition state conformational effect on the activation energy of ethyl acetate neutral hydrolysis. *Heliyon* 5: e02409.

Fei, Z., Yang, W., Mingyuan, Z. & Lihua, K. 2015. C-doped boron nitride fullerene as a novel catalyst for acetylene hydrochlorination: A DFT study. *RSC Advances* 5: 56348-56355.

Francis, A.C. & Richard, J.S. 2007. *Advanced Organic Chemistry. Part A: Structure and Mechanisms.* New York: Springer.

Frisch, M.J., Trucks, G.W., Schlegel, H.B., Scuseria, G.E., Robb, M.A., Cheeseman, J.R., Scalmani, G., Barone, V., Mennucci, B., Petersson, G.A., Nakatsuji, H., Caricato, M., Li, X., Hratchian, H.P., Izmaylov, A.F., Bloino, J., Zheng, G., Sonnenberg, J.L., Hada, M., Ehara, M., Toyota, K., Fukuda, R., Hasegawa, J., Ishida, M., Nakajima, T., Honda, Y., Kitao, O., Nakai, H., Vreven, T., Montgomery Jr., J.A., Peralta, J.E., Ogliaro, F., Bearpark, M., Heyd, J.J., Brothers, E., Kudin, K.N., Staroverov, V.N., Kobayashi, R., Normand, J., Raghavachari, K., Rendell, A., Burant, J.C., Iyengar, S.S., Tomasi, J., Cossi, M., Rega, N., Millam, J.M., Klene, M., Knox, J.E., Cross, J.B., Bakken, V., Adamo, C., Jaramillo, J., Gomperts, R., Stratmann, R.E., Yazyev, O., Austin, A.J., Cammi, R., Pomelli, C., Ochterski, J.W., Martin, R.L., Morokuma, K., Zakrzewski, V.G., Voth, G.A., Salvador, P., Dannenberg, J.J., Dapprich, S., Daniels, A.D., Farkas, O., Foresman, J.B., Ortiz, J.V., Cioslowski, J. & Fox, D.J. 2010. *Gaussian 09, Revision B.01*. Wallingford: Gaussian Inc.

Hossein, T., Mohammad, A.R. & Amir, M. 2019. DFT study on the mechanistic details of the hydrolysis of dicyan using acetaldehyde as the first organocatalyst. *Computational and Theoretical Chemistry* 1154: 37-43.

Hui, Z., Yan, S., Hong, Z., Xuan, W., Han, B. & Zesheng, L. 2019. Further discussion on the reaction behaviour of triallyl isocyanurate in the UV radiation cross-linking process of polyethylene: A theoretical study. *Royal Society Open Science* 6: 182196.

Hussein, A.A., Al-Hadedi, A.A.M., Mahrath, A.J., Moustafa, G.A.I., Almalki, F.A., Alqahtani, A., Shityakov, S. & Algazally, M.E. 2020. Mechanistic investigations on pinnick oxidation: A density functional theory study. *Royal Society Open Science* 7: 191568.

Jae, S.L. & Young, C.P. 2014. Stability and interconversion of acetylcholine conformers. *Bulletin of the Korean Chemical Society* 35(10): 2911-2916.

Johannes, K., Peter, B. & Ulrich, S. 2016. Assessment of different basis sets and DFT functionals for the calculation of structural parameters, vibrational modes and ligand binding energies of Zr4O2(carboxylate)12 clusters. *Computational and Theoretical Chemistry* 22: 127-135.

Johannes, Z., Helmut, H., Joseph, D.S. & Miroslaw, C. 1997. Selectivity of lipases: Con- formational analysis of suggested intermediates in ester hydrolysis of chiral primary and secondary alcohols. *Journal of Molecular Catalysis B: Enzymatic* 3: 83-98.

John, R. & William, J.G. 1934. Researches in the menthone series. Part XIII. The relative molecular configurations of the menthols and menthylamines. *Journal of the Chemical Society* 1934: 1779-1783.

Joseph, W.O., Petersson, G.A. & Montgomery, J.A. 1996. A complete basis set model chemistry. V. Extensions to six or more heavy atoms. *Journal of Chemical Physics* 104: 2598.

Juan, R.A. & Annia, G. 2010. Counterpoise corrected interaction energies are not systematically better than uncorrected ones: Comparison with CCSD(T) CBS extrapolated values. *Theoretical Chemistry Accounts* 126: 75-85.

Kuchitsu, K. 1998. *Structure of Free Polyatomic Molecules: (Basic) Data*. 1st ed. Berlin: Springer-Verlag Berlin Heidelberg.

Nadezhda, R.K., Vladimir, F.M., Dmitry, B.K., Ekaterina, V.M. & Oleg, I.G. 2016. Synthesis, crystal structure and hydrolysis of novel isomeric cage (p{c/p{o)-phosphoranes on the basis of 4,4,5,5-tetramethyl-2-(2-oxo-1,2-diphenylethoxy)-1,3,2-dioxaphospholane and hexafluoroacetone. *RSC Advances* 6: 85745-85755.

Nina, N.C., Nataliya, F.L., Larisa, P.O., Igor, M.L. & Bagrat, A.S. 2015. The hydrolysis of (o{si)-chelate [n-(acetamido) methyl] dimethylchlorosilanes. DFT and MP2 study, QTAIM and NBO analysis. *Computational and Theoretical Chemistry* 1070: 162-173.

Petersson, G.A., Andrew, B., Thomas, G.T., Mohammad, A.A. & William, A.S. 1988. A complete basis set model chemistry. I. The total energies of closed-shell atoms and hydrides of the first-row elements. *The Journal of Chemical Physics* 89: 2193-2218.

Deslongchamps, P. 1975. The importance of conformation of the tetrahedral intermediate in the hydrolysis of esters and amides. In *Organic Syntheses*, edited by Bruylants, A., Ghosez, L. & Viehe, H.G. Oxford: Butterworth-Heinemann. pp. 351-378.

Pierre, H. & Walter, K. 1964. Inhomogeneous electron. *Physical Review* 136: B864-B871.

Radhakrishnamurti, P.S. & Prakash, C.P. 1970. Conformational studies in ester hydrolysis. *Proceedings of the Indian Academy of Sciences Section A* 71: 181-188.

Rincón, D.A., D.S. Cordeiro, M.N. & Mosquera, R.A. 2016. On the effects of the basis set superposition error on the change of QTAIM charges in adduct formation. Application to complexes between morphine and cocaine and their main metabolites. *RSC Advances* 6: 110642-110655.

Rizka, N.F., Febdian, R., Nufida, D.A., Vera, K., Hermawan, K.D., Faozan, A., Mudasir, & Ira, P. 2020. A density functional study of the preference of acetylcholine in the neutral hydrolysis. *Molecules* 25: 670.

Roman, M.B. 2010. Communications: Intramolecular basis set superposition error as a measure of basis set incompleteness: Can one reach the basis set limit without extrapolation? *The Journal of Physical Chemistry* 132: 211103.

Santanu, M., Shree, S.V.S. & Raghavan, B.S. 2018. A quantification scheme for non-covalent interactions in the enantio-controlling transition states in asymmetric catalysis. *Organic & Biomolecular Chemistry* 16: 5643-5652.

Simone, G., Giovanna, L., Sergio, A., Stefan, E.B. & David, A.L. 2019. Bilirubin and its congeners: Conformational analysis and chirality from metadynamics and related computational methods. *Monatshefte für Chemie - Chemical Monthly* 150: 801-812.

Takeshi, Y., David, P.T. & Nicholas, C.H. 2004. A new hybrid exchange–correlation functional using the coulomb-attenuating method (cam- b3lyp). *Chemical Physics Letter* 393: 51-57.

Toby, T., Qingfeng, P., Luke, S., Ian, C., Wenhui, Z., Xiaocong, W., Robert, J.W. & Anthony, S.S. 2017. O-acetyl side-chains in monosaccharides: Redundant nmr spin- couplings and statistical models for acetate ester conformational analysis. *Journal of Physical Chemistry B* 121: 66-77.

Venkatasubban, K.S., Kenneth, R.D. & John, L.H. 1978. Transition-state structure for the neutral water-catalyzed hydrolysis of ethyl trifluorothiolacetate. *Journal of the American Chemical Society* 78: 6125-6128.

Venkatesan, V., Polke, B.G. & Sikder, A.K. 2012. *Ab initio* study on the intermolecular interactions between 1,1-diamino-2,2-dinitroethylene and acetylene: Pull effect on complex formation. *Computational and Theoretical Chemistry* 995: 49-54.

Vladimir, K. & Nediljko, B. 2018. Hydrolysis, polarity, and conformational impact of C terminal partially fluorinated ethyl esters in peptide models. *Beilstein Journal of Organic Chemistry* 13: 2452-2457.

Walter, K. & Lu, J.S. 1965. Self-consistent equations including exchange and correlation effects. *Physical Reviews* 140: A1133-A1138.

Weck, C., Nauha, E. & Gruber, T. 2019. Does the exception prove the rule? A comparative study of supramolecular synthons in a series of lactam esters. *Crystal Growth & Design* 19: 2899-2911.

William, M.H. 2015. *CRC Handbook of Chemistry and Physics*. Florida: CRC Press. pp. 1-2677.

Yan, Z. & Donald, G.T. 2008. The M06 suite of density functionals for main group thermochemistry, thermochemical kinetics, noncovalent interactions, excited states, and transition elements: two new functionals and systematic testing of four M06-class functionals and 12 other functionals. *Theoretical Chemistry Accounts* 120: 215-241.

Young, D.C. 2001. *Computational Chemistry: A Practical Guide for Applying Techniques to Real-World Problems*. New York: Wiley. pp. 1-398.

Yuan, L., Jijun, Z., Fengyu, L. & Zhongfang, C. 2013. Appropriate description of intermolecular interactions in the methane hydrates: An assessment of DFT methods. *Journal of Computational Chemistry* 34: 121-131.

*Corresponding author; email: rusydi@fst.unair.ac.id

Formula for calculating average and span of ΔE_{13}

$$\text{Average} = \frac{\sum_{n=1}^{9} \Delta E_{13}}{9} \quad (1)$$

$$\text{Span} = \Delta E_{13\text{highest}} - \Delta E_{13\text{lowest}} \quad (2)$$

CARTESIAN COORDINATES OF THE OPTIMIZED GROUND STATE

THE PREDICTION OF DFT (M4)

Table S1. The Cartesian coordinate of the optimized Et1(1)

Atom	x (Å)	y (Å)	z (Å)
C	-1.412588000	0.454941000	-0.000164000
O	-1.942013000	-0.632771000	-0.000263000
H	-1.951937000	1.413388000	-0.000204000
O	-0.092134000	0.688187000	0.000011000
C	0.774375000	-0.480943000	0.000086000
C	2.207990000	0.012040000	0.000274000
H	0.542631000	-1.080961000	-0.884876000
H	0.542414000	-1.081009000	0.884959000
H	2.890020000	-0.844569000	0.000329000
H	2.415799000	0.616823000	-0.887411000
H	2.415585000	0.616767000	0.888048000

Table S2. The Cartesian coordinate of the optimized Et1(2)

Atom	x (Å)	y (Å)	z (Å)
C	1.336005000	-0.209976000	-0.255522000
O	1.527164000	0.886343000	0.219475000
H	2.080966000	-0.777889000	-0.831542000
O	0.206398000	-0.929027000	-0.167625000
C	-0.906258000	-0.338503000	0.564201000
C	-1.765858000	0.524387000	-0.346296000
H	-0.506163000	0.236408000	1.402468000
H	-1.459870000	-1.200305000	0.942339000
H	-2.633998000	0.891986000	0.211825000
H	-1.204715000	1.388513000	-0.711663000
H	-2.128044000	-0.052700000	-1.202534000

TABLE S3. The Cartesian coordinate of the optimized Et2(1-a)

Atom	x (Å)	y (Å)	z (Å)
C	1.042820000	0.143516000	-0.000038000
C	2.140931000	-0.891907000	0.000035000
H	2.051813000	-1.533460000	-0.881985000
H	3.109609000	-0.392718000	0.000314000
H	2.051435000	-1.533807000	0.881759000
C	-2.572906000	-0.401100000	0.000128000
C	-1.321020000	0.455369000	-0.000015000
H	-3.458604000	0.242923000	0.000046000
H	-2.612662000	-1.039920000	-0.887379000
H	-2.612638000	-1.039659000	0.887825000
H	-1.261098000	1.097305000	-0.884200000
H	-1.261073000	1.097563000	0.883980000
O	1.210353000	1.346636000	-0.000229000
O	-0.178569000	-0.438322000	0.000100000

TABLE S4. The Cartesian coordinate of the optimized Et2(2-d)

Atom	x (Å)	y (Å)	z (Å)
C	-0.914021000	0.174263000	-0.052811000
C	-2.215739000	-0.499093000	0.307477000
H	-2.096975000	-1.063783000	1.237528000
H	-2.992823000	0.255077000	0.429619000
H	-2.501186000	-1.210841000	-0.472746000
C	2.204100000	0.052611000	0.636304000
C	1.380713000	-0.237425000	-0.609551000
H	3.214561000	0.361168000	0.345675000
H	1.755942000	0.860782000	1.220461000
H	2.286177000	-0.838742000	1.266129000
H	1.265010000	0.655855000	-1.227732000
H	1.824418000	-1.038995000	-1.204503000
O	-0.748100000	1.374150000	-0.144665000
O	0.062420000	-0.739482000	-0.265704000

TABLE S5. The cartesian coordinate of the optimized Et3(1-d)

Atom	x (Å)	y (Å)	z (Å)
C	0.635921000	0.616828000	-0.000050000
C	1.991595000	-0.073247000	0.000067000
H	2.540597000	0.246163000	-0.891490000
H	2.540490000	0.246258000	0.891656000
F	1.911118000	-1.459590000	0.000137000
C	-2.731622000	-0.759610000	0.000084000
C	-1.722908000	0.371678000	-0.000103000
H	-3.744934000	-0.344644000	0.000018000
H	-2.616579000	-1.388713000	-0.887324000
H	-2.616575000	-1.388420000	0.887700000
H	-1.811715000	1.008202000	-0.885285000
H	-1.811713000	1.008497000	0.884867000
O	0.556416000	1.829449000	-0.000164000
O	-0.396109000	-0.227564000	-0.000007000

TABLE S6. The Cartesian coordinate of the optimized Et3(2-e)

Atom	x (Å)	y (Å)	z (Å)
C	-0.454668000	0.557274000	-0.070216000
C	-1.917879000	0.242728000	0.202070000
H	-2.159205000	0.578345000	1.215765000
H	-2.528158000	0.801470000	-0.514593000
F	-2.228212000	-1.106401000	0.094903000
C	2.508120000	-0.366226000	0.657092000
C	1.694584000	-0.310564000	-0.625891000
H	3.573625000	-0.282676000	0.416388000
H	2.244679000	0.458309000	1.324967000
H	2.347696000	-1.313923000	1.179811000
H	1.813830000	0.646682000	-1.138077000
H	1.953985000	-1.126115000	-1.303683000
O	-0.049844000	1.702412000	-0.020640000
O	0.278159000	-0.520381000	-0.355990000

TABLE S7. The Cartesian coordinate of the optimized Et1(1)

Atom	x (Å)	y (Å)	z (Å)
C	1.403491000	0.450036000	-0.000004000
O	1.913104000	-0.637569000	-0.000011000
H	1.949296000	1.404510000	-0.000011000
O	0.086149000	0.700635000	0.000013000
C	-0.751514000	-0.473596000	0.000020000
C	-2.192371000	0.003896000	-0.000016000
H	-0.520411000	-1.075306000	0.885198000
H	-0.520377000	-1.075342000	-0.885125000
H	-2.868387000	-0.858458000	-0.000005000
H	-2.395908000	0.609051000	0.889172000
H	-2.395878000	0.609005000	-0.889242000

TABLE S8. The cartesian coordinate of the optimized Et1(2)

Atom	x (Å)	y (Å)	z (Å)
C	1.314157000	-0.185485000	-0.244859000
O	1.442146000	0.904619000	0.244294000
H	2.091359000	-0.714793000	-0.814425000
O	0.218741000	-0.957742000	-0.187726000
C	-0.899003000	-0.398675000	0.535740000
C	-1.692836000	0.566656000	-0.333758000
H	-0.529317000	0.095621000	1.438229000
H	-1.498975000	-1.267032000	0.816733000
H	-2.585255000	0.902266000	0.207123000
H	-1.089044000	1.442773000	-0.585492000
H	-2.009776000	0.071181000	-1.257447000

TABLE S9. The cartesian coordinate of the optimized Et2(1-a)

Atom	x (Å)	y (Å)	z (Å)
C	-1.032067000	0.148920000	0.000008000
C	-2.136653000	-0.883785000	-0.000004000
H	-2.041134000	-1.521401000	0.884422000
H	-3.103874000	-0.379378000	0.000143000
H	-2.041305000	-1.521190000	-0.884601000
C	2.557802000	-0.399155000	0.000003000
C	1.300233000	0.451731000	-0.000011000
H	3.443277000	0.246489000	-0.000014000
H	2.589241000	-1.037223000	0.889104000
H	2.589235000	-1.037261000	-0.889071000
H	1.243280000	1.094533000	0.884801000
H	1.243277000	1.094498000	-0.884849000
O	-1.185655000	1.344310000	0.000003000
O	0.178418000	-0.449977000	0.000009000

TABLE S10. The Cartesian coordinate of the optimized Et2(2-d)

Atom	x (Å)	y (Å)	z (Å)
C	-0.885345000	0.174584000	-0.069170000
C	-2.213815000	-0.426713000	0.330640000
H	-2.108253000	-0.929278000	1.297373000
H	-2.963405000	0.362904000	0.397241000
H	-2.514257000	-1.177394000	-0.406451000
C	2.142878000	0.142447000	0.634365000
C	1.364000000	-0.342151000	-0.581046000
H	3.169288000	0.393308000	0.341816000
H	1.674146000	1.034824000	1.058141000
H	2.179407000	-0.641950000	1.397937000
H	1.276013000	0.447253000	-1.332336000
H	1.835201000	-1.220100000	-1.029674000
O	-0.670422000	1.348874000	-0.238791000
O	0.046116000	-0.793695000	-0.212807000

TABLE S11. The cartesian coordinate of the optimized Et3(1-d)

Atom	x (Å)	y (Å)	z (Å)
C	0.627156000	0.614379000	-0.000064000
C	1.986801000	-0.069813000	0.000054000
H	2.526750000	0.263543000	-0.891958000
H	2.526698000	0.263747000	0.892021000
F	1.904795000	-1.439603000	0.000208000
C	-2.717684000	-0.755062000	0.000055000
C	-1.697920000	0.368774000	-0.000090000
H	-3.729724000	-0.334908000	-0.000019000
H	-2.597085000	-1.382141000	-0.888880000
H	-2.597110000	-1.381889000	0.889171000
H	-1.788311000	1.005939000	-0.885740000
H	-1.788335000	1.006191000	0.885375000
O	0.530726000	1.816615000	-0.000211000
O	-0.391496000	-0.245831000	0.000015000

TABLE S12. The Cartesian coordinate of the optimized Et3(2-e)

Atom	x (Å)	y (Å)	z (Å)
C	-0.423992000	0.537829000	-0.092815000
C	-1.898322000	0.288328000	0.191385000
H	-2.114722000	0.681605000	1.189790000
H	-2.478032000	0.849285000	-0.548537000
F	-2.246240000	-1.037640000	0.136958000
C	2.459013000	-0.282459000	0.677514000
C	1.663334000	-0.407300000	-0.613902000
H	3.530201000	-0.244541000	0.447939000
H	2.185252000	0.632343000	1.210337000
H	2.270226000	-1.146398000	1.323259000
H	1.796057000	0.472567000	-1.248846000
H	1.940774000	-1.305535000	-1.169518000
O	0.030991000	1.655492000	-0.084484000
O	0.254785000	-0.582861000	-0.341783000

CARTESIAN COORDINATES OF THE OPTIMIZED TRANSITION STATE

THE PREDICTION OF DFT (M4)

TABLE S13. The cartesian coordinate of the optimized [Et1(1)–water]

Atom	x (Å)	y (Å)	z (Å)
C	1.341192000	-0.316936000	0.391323000
O	1.534384000	-1.201157000	-0.393535000
H	1.756515000	-0.158017000	1.387119000
O	-0.257252000	0.204648000	0.622036000
C	-1.259562000	-0.564201000	-0.071616000
C	-2.540610000	0.249597000	-0.175147000
H	-1.418818000	-1.480034000	0.506502000
H	-0.883041000	-0.851276000	-1.060155000
H	-3.317552000	-0.344215000	-0.668878000
H	-2.903259000	0.536996000	0.816109000
H	-2.385559000	1.160325000	-0.763394000
O	1.464622000	1.320971000	-0.223692000
H	1.688251000	1.231372000	-1.163703000
H	0.283318000	1.098391000	0.040569000

TABLE S14. The Cartesian coordinate of the optimized [Et1(2)–water]

Atom	x (Å)	y (Å)	z (Å)
C	-1.041784000	0.520522000	0.453311000
O	-0.991239000	1.440208000	-0.313409000
H	-1.261676000	0.507081000	1.520997000
O	0.182319000	-0.654108000	0.353947000
C	1.256916000	-0.349108000	-0.557087000
C	2.468454000	0.154067000	0.211699000
H	0.906171000	0.400864000	-1.276535000
H	1.485664000	-1.273151000	-1.098798000
H	3.294739000	0.353714000	-0.479679000
H	2.234393000	1.084306000	0.738416000
H	2.800149000	-0.587223000	0.944999000
O	-1.991299000	-0.863017000	-0.043383000
H	-2.348215000	-0.635404000	-0.916736000
H	-0.810987000	-1.187727000	-0.057441000

TABLE S15. The Cartesian coordinate of the optimized [Et2(1-a)–water]

Atom	x (Å)	y (Å)	z (Å)
C	-1.111102000	-0.227655000	0.195979000
C	-2.046230000	-0.460093000	-0.949270000
H	-1.972301000	-1.512013000	-1.239749000
H	-3.063801000	-0.252126000	-0.608477000
H	-1.802185000	0.175856000	-1.797926000
C	2.838682000	0.170058000	-0.155705000
C	1.560451000	-0.612181000	0.117086000
H	3.683916000	-0.307287000	0.352446000
H	3.055855000	0.204856000	-1.227568000
H	2.759992000	1.198714000	0.212860000
H	1.654171000	-1.645055000	-0.237044000
H	1.334882000	-0.644758000	1.190638000
O	-1.075498000	-0.718508000	1.285332000
O	0.458527000	-0.019061000	-0.583513000
O	-0.925855000	1.573013000	0.198417000
H	0.104137000	1.067629000	-0.231981000
H	-0.862858000	1.809862000	1.136369000

TABLE S16. The Cartesian coordinate of the optimized [Et2(2-d)–water]

Atom	x (Å)	y (Å)	z (Å)
C	-0.925758000	-0.281413000	0.296088000
C	-1.562840000	-1.292992000	-0.604341000
H	-1.000548000	-2.227063000	-0.517631000
H	-2.588549000	-1.457467000	-0.264203000
H	-1.565541000	-0.958174000	-1.639821000
C	2.631637000	-0.510170000	-0.093220000
C	1.616039000	0.605918000	0.102539000
H	3.549721000	-0.286877000	0.461928000
H	2.237194000	-1.462693000	0.274659000
H	2.884761000	-0.624937000	-1.151710000
H	1.348706000	0.707889000	1.162827000
H	2.015362000	1.565709000	-0.246097000
O	-0.747027000	-0.291257000	1.478152000
O	0.426726000	0.338025000	-0.654141000
O	-1.592742000	1.278490000	-0.333460000
H	-0.419174000	1.183522000	-0.665674000
H	-1.712057000	1.829976000	0.454913000

TABLE S17. The Cartesian coordinate of the optimized [Et3(1-d)–water]

Atom	x (Å)	y (Å)	z (Å)
C	0.737149000	0.609246000	-0.178620000
C	1.841538000	-0.305733000	-0.667824000
H	1.691787000	-0.468072000	-1.739951000
H	2.797156000	0.196135000	-0.491360000
F	1.860683000	-1.536906000	-0.033019000
C	-3.008636000	-0.632318000	0.050838000
C	-1.848839000	0.230065000	-0.421448000
H	-3.953203000	-0.208423000	-0.306987000
H	-2.918510000	-1.652681000	-0.332476000
H	-3.049446000	-0.677296000	1.144164000
H	-1.807740000	0.279520000	-1.513847000
H	-1.925802000	1.255529000	-0.042972000
O	0.550982000	1.728701000	-0.589502000
O	-0.611930000	-0.364145000	0.024739000
O	0.775917000	0.444607000	1.549301000
H	-0.237892000	-0.119081000	1.137084000
H	0.610467000	1.345657000	1.869534000

TABLE S18. The cartesian coordinate of the optimized [Et3(2-e)–water]

Atom	x (Å)	y (Å)	z (Å)
C	0.718079000	-0.260875000	0.356848000
C	1.637362000	0.686727000	-0.383438000
H	2.651733000	0.555696000	0.002512000
H	1.600736000	0.515659000	-1.458463000
F	1.228884000	1.994340000	-0.121709000
C	-2.561647000	0.834428000	-0.040167000
C	-1.896204000	-0.531035000	-0.004101000
H	-3.541027000	0.783565000	0.448316000
H	-1.953764000	1.574871000	0.487770000
H	-2.704136000	1.172312000	-1.070949000
H	-1.742281000	-0.870949000	1.026625000
H	-2.486659000	-1.281678000	-0.539362000
O	0.502406000	-0.342151000	1.531510000
O	-0.613937000	-0.473911000	-0.667225000
O	1.174015000	-1.791620000	-0.466913000
H	0.012561000	-1.460464000	-0.796531000
H	1.217482000	-2.452088000	0.241638000

TABLE S19. The Cartesian coordinate of the optimized [Et1(1)–water]

Atom	x (Å)	y (Å)	z (Å)
C	1.297169000	-0.301547000	0.437154000
O	1.463134000	-1.246720000	-0.273269000
H	1.677750000	-0.103226000	1.440440000
O	-0.262135000	0.291930000	0.567901000
C	-1.198374000	-0.441022000	-0.232300000
C	-2.577910000	0.176687000	-0.063256000
H	-1.180839000	-1.483196000	0.102090000
H	-0.885275000	-0.427430000	-1.284342000
H	-3.314598000	-0.387775000	-0.646695000
H	-2.874687000	0.160947000	0.990024000
H	-2.583611000	1.215762000	-0.410236000
O	1.540193000	1.238385000	-0.272973000
H	1.743070000	1.040197000	-1.194047000
H	0.363352000	1.111242000	-0.020097000

TABLE S20. The Cartesian coordinate of the optimized [Et1(2)–water]

Atom	x (Å)	y (Å)	z (Å)
C	-0.969575000	0.530104000	0.440451000
O	-0.798446000	1.423058000	-0.335860000
H	-1.225327000	0.566331000	1.500280000
O	0.135438000	-0.726698000	0.421239000
C	1.208989000	-0.522214000	-0.506952000
C	2.340971000	0.235994000	0.169492000
H	0.839697000	0.034608000	-1.376631000
H	1.533867000	-1.515704000	-0.833546000
H	3.184519000	0.349674000	-0.521474000
H	2.001252000	1.232940000	0.467234000
H	2.682248000	-0.304766000	1.058253000
O	-2.007250000	-0.721973000	-0.075701000
H	-2.249563000	-0.461719000	-0.971661000
H	-0.886939000	-1.159763000	-0.017825000

TABLE S21. The Cartesian coordinate of the optimized [Et2(1-a)–water]

Atom	x (Å)	y (Å)	z (Å)
C	1.079195000	-0.221973000	-0.195389000
C	1.930323000	-0.660540000	0.961620000
H	1.748928000	-1.726579000	1.128707000
H	2.978381000	-0.506707000	0.689546000
H	1.690003000	-0.094642000	1.861227000
C	-2.861752000	0.005353000	0.293324000
C	-1.532362000	-0.319501000	-0.372604000
H	-3.691708000	-0.273248000	-0.366773000
H	-2.959154000	-0.544457000	1.234757000
H	-2.934663000	1.077092000	0.508950000
H	-1.454931000	-1.387166000	-0.605849000
H	-1.420699000	0.230280000	-1.316794000
O	1.060877000	-0.605317000	-1.323977000
O	-0.468920000	0.016537000	0.520190000
O	1.071733000	1.524495000	-0.026846000
H	0.001753000	1.085892000	0.327853000
H	1.040138000	1.833789000	-0.938273000

TABLE S22. The Cartesian coordinate of the optimized [Et2(2-d)–water]

Atom	x (Å)	y (Å)	z (Å)
C	-0.848875000	-0.274858000	0.278606000
C	-1.529887000	-1.265284000	-0.621419000
H	-0.921973000	-2.174859000	-0.643382000
H	-2.512078000	-1.492237000	-0.197108000
H	-1.639907000	-0.865704000	-1.629206000
C	2.476080000	-0.558653000	-0.030355000
C	1.583998000	0.674122000	-0.022014000
H	3.429756000	-0.340832000	0.464931000
H	1.989068000	-1.379722000	0.505757000
H	2.676402000	-0.874531000	-1.059618000
H	1.351975000	0.969129000	1.009631000
H	2.068289000	1.516776000	-0.528520000
O	-0.565802000	-0.358725000	1.435036000
O	0.371771000	0.403087000	-0.728130000
O	-1.606724000	1.237848000	-0.158989000
H	-0.490663000	1.215053000	-0.610701000
H	-1.632723000	1.717290000	0.675965000

TABLE S23. The Cartesian coordinate of the optimized [Et3(1-d)–water]

Atom	x (Å)	y (Å)	z (Å)
C	0.718896000	0.596091000	-0.199528000
C	1.801063000	-0.343148000	-0.688387000
H	1.605094000	-0.549937000	-1.745435000
H	2.760314000	0.170341000	-0.573829000
F	1.828683000	-1.523775000	0.008504000
C	-2.976281000	-0.673329000	-0.004104000
C	-1.826897000	0.281142000	-0.286888000
H	-3.926593000	-0.207267000	-0.289199000
H	-2.850619000	-1.598939000	-0.574156000
H	-3.018705000	-0.924709000	1.061234000
H	-1.773450000	0.547265000	-1.347023000
H	-1.932601000	1.213683000	0.281592000
O	0.505637000	1.693328000	-0.643270000
O	-0.597044000	-0.369308000	0.063882000
O	0.829940000	0.499526000	1.489620000
H	-0.166577000	-0.093042000	1.140034000
H	0.636033000	1.403677000	1.761828000

TABLE S24. The Cartesian coordinate of the optimized [Et3(2-e)–water]

Atom	x (Å)	y (Å)	z (Å)
C	0.677567000	-0.242329000	0.332313000
C	1.524435000	0.817878000	-0.326963000
H	2.487481000	0.829335000	0.162113000
H	1.627184000	0.638957000	-1.383818000
F	0.915035000	2.020942000	-0.137767000
C	-2.443607000	0.716101000	0.012055000
C	-1.820116000	-0.658350000	-0.100845000
H	-3.459696000	0.624224000	0.383937000
H	-1.880559000	1.336075000	0.698717000
H	-2.470006000	1.204221000	-0.955903000
H	-1.759450000	-1.146503000	0.861689000
H	-2.368626000	-1.287869000	-0.789314000
O	0.452130000	-0.355687000	1.485869000
O	-0.500478000	-0.551373000	-0.643853000
O	1.338070000	-1.647629000	-0.425904000
H	0.157203000	-1.451883000	-0.808165000
H	1.483710000	-2.297324000	0.242388000